Environmental Science & Technology

pubs.acs.org/est

Article

Redox Heterogeneities Promote Thioarsenate Formation and Release into Groundwater from Low Arsenic Sediments

Naresh Kumar, Vincent Noël, Britta Planer-Friedrich, Johannes Besold, Juan Lezama-Pacheco, John R. Bargar, Gordon E. Brown, Jr., Scott Fendorf, and Kristin Boye*

Cite This: *Environ. Sci. Technol.* 2020, 54, 3237−3244

Read Online

ACCESS | Metrics & More | Article Recommendations | Supporting Information

ABSTRACT: Groundwater contamination by As from natural and anthropogenic sources is a worldwide concern. Redox heterogeneities over space and time are common and can influence the molecular-level speciation of As, and thus, As release/retention but are largely unexplored. Here, we present results from a dual-domain column experiment, with natural organic-rich, fine-grained, and sulfidic sediments embedded as lenses (referred to as "reducing lenses") within natural aquifer sand. We show that redox interfaces in sulfur-rich, alkaline aquifers may release concerning levels of As, even when sediment As concentration is low (<2 mg/kg), due to the formation of mobile thioarsenates at aqueous sulfide/Fe molar ratios <1. In our experiments, this behavior occurred in the aquifer sand between reducing lenses and was attributed to the spreading of sulfidic conditions and subsequent Fe reductive dissolution. In contrast, inside reducing lenses (and some locations in the aquifer) the aqueous sulfide/Fe molar ratios exceeded 1 and aqueous sulfide/As molar ratios exceeded 100, which partitioned As(III)−S to the solid phase (associated with organics or as realgar (As_4S_4)). These results highlight the importance of thioarsenates in natural sediments and indicate that redox interfaces and sediment heterogeneities could locally degrade groundwater quality, even in aquifers with unconcerning solid-phase As concentrations.

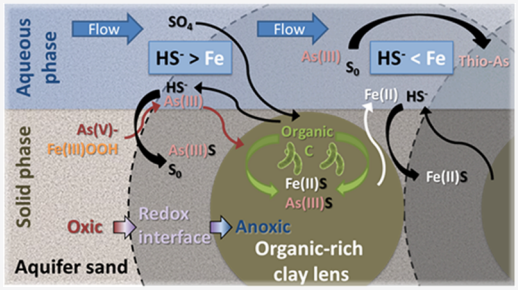

■ INTRODUCTION

Arsenic contamination of groundwater is a major concern globally even where the natural background of As in soils and sediments is low.[1] The mechanisms by which As is released to groundwater depend on how As is bound in the solid phase or adsorbed onto solid surfaces.[2−4] Commonly, As release into the aqueous phase is promoted by redox transformations, such as the development of anaerobic conditions in aquifers rich in Fe(III) hydroxides, oxyhydroxides, and oxides (hereafter collectively referred to as Fe(III) oxides) in the large river deltas in South- and South−East Asia.[3,5] However, the reverse situation can also occur when oxygenated water is injected into anoxic aquifers with As-containing minerals such as arsenopyrite, although this can lead simply to the repartitioning of arsenic onto newly formed Fe(III) oxides.[6−8]

The mobility of As is particularly challenging to predict in heterogeneous redox environments due to its ability to adsorb to and/or co-precipitate with both Fe(III) oxides and sulfides, as well as to form a variety of aqueous As-containing species, including As-oxoanions (arsenate and arsenite), as well as methylated and/or thiolated As, all with varying chemical properties. The occurrence of thiolated As in aquatic systems with elevated As concentrations has been increasingly noted, particularly in environments rich in organic matter and sulfur.[9−14] Moreover, because As-containing species are among the more naturally abundant toxic species in soils and sediments, the risk of these species entering groundwater at hazardous concentration levels is great even where the background solid-phase concentrations of As are below the global average (1.8 mg/kg). Therefore, there is a critical need to understand how hydrological and redox dynamics influence the dissolved concentrations of As in the naturally occurring heterogeneity of subsurface environments to preserve groundwater resources following changes in water management, land use, or climatic conditions.

Here, our objective is to elucidate the fate of As within a common alluvial aquifer setting: an unconfined, coarse-grained aquifer in contact with fine-grained, organic-rich sediments (often existing as lenses), sometimes referred to as "naturally reduced zones" (NRZs).[15−20] In laboratory flow-through column experiments, we used sediments originating from the Wind River-Little Wind River floodplain near Riverton, WY, exhibiting low sedimentary As concentrations (<2 mg/kg). This floodplain contains high sulfate concentrations and, due to the dry climate, high alkalinity and salinity as well. The

Received: October 28, 2019
Revised: February 16, 2020
Accepted: February 18, 2020
Published: February 18, 2020

Downloaded via STANFORD UNIV on August 4, 2020 at 15:58:39 (UTC).
See https://pubs.acs.org/sharingguidelines for options on how to legitimately share published articles.

ACS Publications © 2020 American Chemical Society

https://dx.doi.org/10.1021/acs.est.9b06502
Environ. Sci. Technol. 2020, 54, 3237−3244

floodplain is representative of alluvial aquifers globally, particularly within arid/semiarid environments. By embedding various numbers of organic-rich, fine-grained, sulfidic lenses in the aquifer sand at various distances along the length of the column, we were able to both determine the influence of reduced zones on the geochemical processes involving As and establish concentration thresholds of As, sulfide, and Fe that regulated the chemical speciation of As in solid and aqueous phases. Our results provide clear evidence of the importance of redox interfaces for controlling As behavior in groundwater aquifers with high S concentrations. Further, we demonstrate the significant influence that fine-grained lenses, which operate as reducing zones, can have on groundwater quality in otherwise coarse-grained, oxic aquifers.

■ MATERIALS AND METHODS

Column Design and Sediment Properties. Detailed descriptions of the column setup are provided in the Supporting Information (SI, pages 2−3), along with initial sediment properties (Supporting Information, pages 2−3 and 7−8, Tables SI-1 and SI-2 and Figure SI-5). Briefly, 12 columns (30 cm long, 7 cm diameter) were filled with natural sediments, collected ∼2 weeks prior from the Wind River-Little Wind River floodplain outside of Riverton, WY (42°59′19.1″N, 108°23′58.6″W). Triplicate columns were set up with 0 (control), 1, 2, or 3 fine-grained, organic-rich, reducing lens(es) (∼3 cm diameter, 17−20 g dry weight each) embedded in aquifer sand (1.3−1.4 kg dry sand per column) at increasing distances (with each additional lens) from the influent (bottom) groundwater port. The lenses consisted of organic-rich, fine-grained, sulfidic sediments collected underneath an oxbow lake on the floodplain and thoroughly homogenized to ensure consistent composition between different lenses. The As concentrations in aquifer sand and oxbow lake sediment materials were 1.2 ± 0.4 and 0.7 ± 0.1 mg As/kg sediment, respectively. Porewater samplers (Rhizon-Flex, 5 cm, 0.15 μm pore size, Rhizosphere Research Products, Wageningen, Netherlands) were inserted into the sand to enable sampling of groundwater (advective zone) before and after fine-grained lens(es) (and at increasing distances away from the reduced zones in columns with one or two lenses) along the flow path. Micro-rhizons (8 mm, 0.15 μm pore size, Rhizosphere Research Products, Wageningen, Netherlands) were inserted into the center of each lens to enable sampling of porewater from the reduced (diffusive) zones. All columns were fed artificial groundwater (by peristaltic pump at a flow rate of 90 mL/day, equivalent to ∼1 pore volume exchange per 48 h) made to have a chemical composition similar in concentrations of the major solutes, except organic C, measured in Riverton floodplain groundwater at the site over the past 2 years (Supporting Information, Table SI-3). The sulfate concentrations in the groundwater at this site are high relative to elsewhere in the Riverton area,[21] but we preferred to use a concentration representative of the site. The artificial groundwater was fully aerated (240−260 μM dissolved O_2) in the source container to achieve a dissolved oxygen concentration in the control columns (∼50 μM) similar to that measured in the floodplain groundwater (average 87 μM, range 14−211 μM). Finally, the artificial groundwater had a pH of ∼8, which is higher than that recently measured at the floodplain site, but within the normal range of groundwater in the area.[21]

Experimental Details. The column experiment was run for a total of 70 days. Porewater from the rhizons and micro-rhizons was sampled every 7 days using prerinsed 3 mL luer lock syringes. To flush the tubing, the first 1−3 mL of water extracted from rhizons was discarded. PEEK tubing connected to micro-rhizons was assumed to have minimal contribution to the porewater samples obtained from these ports. Dissolved sulfide was always analyzed on the second, freshly extracted sample from micro-rhizons (the first sample being used for total element concentrations).

Aqueous Phase Analyses. The aqueous phase in this study is defined as containing all colloidal and dissolved species <0.15 μm, by virtue of the pore size of the porewater samplers. Total aqueous concentrations of S and Fe were determined by inductively coupled plasma optical emission spectroscopy (ICP-OES, iCAP6000, Thermo Scientific, Cambridge, U.K.) and total aqueous As by inductively coupled plasma mass spectrometry (ICP-MS, XSERIES 2, Thermo Scientific, Cambridge, U.K.). All ICP analyses were conducted on samples diluted 1:20 with 2% nitric acid, and a reference standard with known S, As, and Fe concentrations was intercalated every 15 samples to monitor instrument drift and concentration retrieval accuracy. No interference from Ar−Cl on As concentrations was detected. Dissolved sulfide (HS^-) concentrations were measured, from day 35 onward, using the methylene blue method[22] on freshly drawn samples that were immediately mixed with the first (stabilizing) reagent to minimize volatilization and exposure to oxygen. Total concentrations of aqueous Fe (from ICP-OES) were assumed to be equivalent to total aqueous Fe(II) because no increase in Fe(II) concentrations (as measured by the ferrozine method[23]) was detected after reduction with hydroxylamine when we tested this for the first few and the final sampling steps (data not shown).

A set of end-point samples from the rhizons (ports 3, 5, and 7) from columns with reducing lenses were flash-frozen immediately after adding diethylene triamine pentaacetic acid (DPTA) (10 mM) to complex Fe(II) and kept at −80 °C until analyzed for aqueous As speciation. Aqueous As species were separated by IC (Dionex ICS-3000) using an IonPac AS-16/AG-16 4 mm column (gradient program with 2.5−100 mM NaOH at a flow rate of 1.2 mL/min and 50 μL injection volume; without suppressor) and quantified by ICP-MS (XSERIES 2, Thermo-Fisher).[10] It should be noted that the chromatographic analyses with NaOH prevent the detection of thioarsenites as they would experience a ligand-exchange (−OH replacing −SH) and, thus, be transformed to the arsenite oxoanion.[12] Thus, there is a slight risk of overestimating the arsenite concentrations at the expense of thiolated As species. Further, we cannot fully exclude that what is measured as thioarsenates could originally have been thioarsenites that oxidized while sitting in capped vials for a few minutes on an autosampler in ambient air, as reported before.[12] More details about the aqueous As speciation methodology are provided in the Supporting Information.

Solid-Phase Sampling. After the final aqueous sampling time, six columns (two control, two with one reducing lens, one with two reducing lenses, and one with three reducing lenses) were disconnected from the peristaltic pump and immediately transferred into a glove bag (3−4% H_2, balance N_2). Sediments from these columns were sampled around each rhizon and micro-rhizon present in the columns. Subsamples were taken to determine the water content (by weighing before

https://dx.doi.org/10.1021/acs.est.9b06502
Environ. Sci. Technol. 2020, 54, 3237−3244

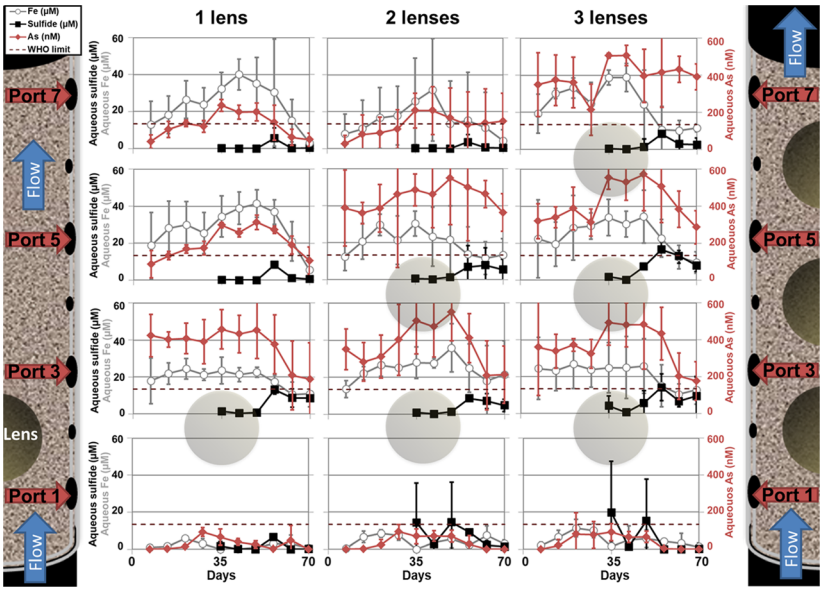

Figure 1. Temporal evolution of aqueous sulfide (μM) and Fe (μM) (both on left vertical axis) and aqueous As (nM, right vertical axis) in the groundwater (horizontal axes) and along the flow path (panels from bottom to top) in columns with 1, 2, or 3 fine-grained, reducing lenses (positions indicated by shaded circles). Values are averages of triplicate columns for each treatment and error bars denote the standard deviation from the mean for the triplicates. The dashed line indicates the WHO drinking water limit for As (10 μg/L = 133.5 nM). To facilitate examining the evaluation of influence from fine-grained, reducing zones on groundwater concentrations, column depth profiles for aqueous As, Fe, and sulfide on days 35 and 70 in the Supporting Information (Figure SI-2).

and after drying at 105 °C) and HCl-extractable Fe(II) (described below). The remainder of the sampled sediments from each port was dried at room temperature and used for HNO_3 digestions (see below).

One of the remaining columns with three reducing lenses was switched over from groundwater solution to glycerol and pumping continued until glycerol had passed through the entire column (i.e., had replaced the groundwater in the advective pores), at which point the column was immediately transferred into the glove bag. This glycerol treatment served to prevent biases in mineral composition and element speciation that could arise from drying and precipitation of evaporite salts. Glycerol preservation also allows for samples to be frozen (a prerequisite for the X-ray absorption analyses, (XAS)) without risking destructive ice formation. Sediment samples were taken around each rhizon and micro-rhizon sampler (as described above) and ground to a smooth paste using an agate mortar and pestle. Samples were stored in 2 mL cryovials inside sealed mason jars with oxygen scrubbers and kept at −20 °C until XAS analyses.

Chemical Extractions. Chemical extractions targeting the reactive Fe(II) pool (HCl-extraction) and total acid-extractable As and Fe were performed on subsamples from all solid-phase samples (not preserved with glycerol).

Reactive Fe(II) Pool: HCl Extraction. Triplicate subsamples equivalent to 1−2 g of dry sediment were weighed into 15 mL centrifuge tubes containing 5 mL of 0.5 M HCl (trace metal grade). After shaking for 2 h, tubes were centrifuged and the supernatant filtered (0.45 μm) into a new 15 mL centrifuge tube. The HCl extracts were analyzed for total Fe concentration (ICP-OES) to compare the concentration of reactive Fe(II) in reducing lenses and aquifer sand before and after the experiment.

Total Acid-Extractable Fraction: Concentrated HNO_3. About 0.2 g of dry sediment was weighed in Teflon tubes and 10 mL of concentrated nitric acid (70% HNO_3, trace metal grade) was added to each tube. Tubes were capped and sediments digested according to the United States EPA standard protocol for total digestion of soil in a CEM MarsXpress microwave digester (CEM, Matthews, NC). Extracts were transferred to acid-washed glass vials and a subsample was diluted 1:5 and analyzed for total Fe by ICP-OES and total As by ICP-MS.

X-ray Absorption Spectroscopy (XAS). *Arsenic X-ray Absorption Near-Edge Structure Spectroscopy (XANES).* Arsenic K-edge XANES spectra of glycerol-preserved end-point samples and the initial aquifer and oxbow lake sediments were collected at 10 K (L-He cryostat) in fluorescence yield mode at BL 7-3 at the Stanford Synchrotron Radiation Lightsource (SSRL). A Si(220) double crystal monochromator was detuned by 50% to minimize higher-order harmonics, and the beam energy was calibrated by setting the first inflection point of a simultaneously measured Au L_{III}-edge to 11,919 eV (double transmission mode). All spectra were averaged and normalized using the Ifeffit 1.2.12 (Matt Newville) Demeter 0.9.25 Athena software (Bruce Ravel).[24] Linear combination least-squares (LC-LS) fitting of the normalized spectra was also performed in Athena. Good fits for all sample spectra were obtained using 2−4 of the following seven standard spectra (out of a comprehensive spectra database): realgar (AsS or As_4S_4), organically complexed $As(III)S_3$ (trisphenylthioarsine), arsenite sorbed to ferrihydrite (Fh) or to mackinawite (FeS), monothioarsenate sorbed to FeS, and arsenate sorbed to Fh or to FeS. More details regarding the As XANES data collection and processing procedures are provided in the Supporting Information.

Sulfur XANES Spectroscopy. Sulfur K-edge XANES spectroscopy was performed in a He atmosphere at SSRL BL 4-3 to compare the solid-phase speciation of S in the initial materials with that of the glycerol-preserved samples. A detailed description of the procedure is provided in the Supporting Information.

https://dx.doi.org/10.1021/acs.est.9b06502
Environ. Sci. Technol. 2020, 54, 3237−3244

RESULTS AND DISCUSSION

Aqueous Phase Chemistry. Aqueous (<0.15 μm colloids and dissolved species) concentrations of As and Fe in aquifer ports (groundwater) increased as a function of time until day 42 of the experiment and were considerably higher in ports immediately downgradient from a fine-grained, reduced lens (Figure 1, Supporting Information Figure SI-2). After day 42, the concentrations of As and Fe decreased again, particularly in ports directly downgradient of reducing lenses. Sulfide was only measured from day 35 of the experiment but generally followed the same pattern as Fe and As. Sulfide and As concentrations always increased directly after a reducing lens, but then decreased with increasing distance from the lenses (Figures 1 and SI-2). In contrast, aqueous Fe concentrations remained elevated independent of the distance from, or the number of, reducing lenses (Figures 1 and SI-2). In an equivalent natural aquifer setting, the large increase in aqueous As from a few nM to >0.5 μM observed in the presence of reducing lenses would be equivalent to a transition from background levels to concentrations exceeding the World Health Organization (WHO) drinking water standard of 10 μg As/L (Figure 1).

In control columns (Supporting Information, Figure SI-3), aqueous concentrations of As in groundwater increased between days 28 and 40, but much less so than in columns with fine-grained, reducing lens(es) (cf. Figure 1). Both aqueous sulfide and Fe concentrations remained close to, or below, the detection limit throughout the experiment in control columns (Supporting Information, Figure SI-3). In contrast to groundwater samples, porewater from inside the lenses exhibited low aqueous Fe concentrations and lower As concentrations but high sulfide concentrations, which were sustained until the end of the experiment (Supporting Information, Figure SI-4).

End-point groundwater samples downgradient of fine-grained, reducing lenses (ports 3, 5, and 7) were analyzed for As speciation (Figure 2). Remarkably large proportions of the aqueous As were in thiolated forms (mono-, di-, and trithioarsenates were observed, with monothioarsenate being most abundant), comprising ∼30−40% of total aqueous As in ports directly downgradient from a lens. Both oxoanions of As, arsenite (AsIII) and arsenate (AsV), were also present in these samples, with the relative abundance of arsenate generally increasing with distance away from the reducing lenses. In port 7 of columns with one or two lens(es), arsenate was the only As species detected (Figure 2).

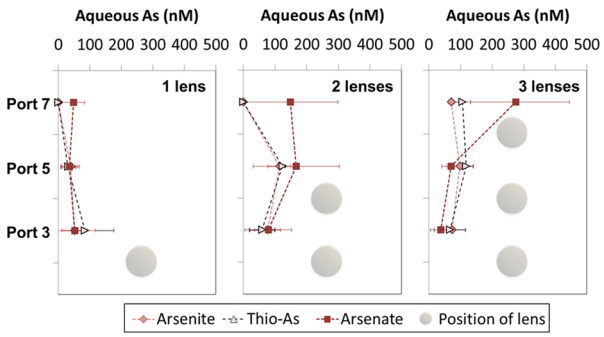

Figure 2. Aqueous concentration of As species (nM) in groundwater at the end of the experiment (day 70). Only water samples taken downgradient from lenses (lens positions are indicated by shaded circles) along the flow path were analyzed for aqueous As species. Values represent averages of triplicate columns for each treatment calculated from the relative distribution between species (normalized to total recovery) multiplied by total aqueous As concentration. Error bars denote the standard deviation of the mean. Thio−As includes mono-, di-, and trithioarsenate species.

Solid-Phase As, Fe, and S Speciation and Spatial Distribution. Acid extractions of the end-point solid-phase samples, as compared to the initial sediments, indicated that large mass transfers of both As and Fe had taken place between fine-grained, reducing lenses and the aquifer material (Figure 3). The HNO_3 digestions showed a net loss of As from all columns that increased with the number of lenses. However, the fine-grained, reducing lenses themselves accumulated As, indicating that aquifer sediment in proximity to lenses was responsible for the net As loss. A slightly different pattern was discerned for Fe, which unlike As was supplied at a low concentration (0.5 mg/L) in the influent groundwater and also was much more abundant in the initial lens material than in the aquifer material (Supporting Information, Table SI-1). Thus, only columns with three reducing lenses exhibited a net loss of Fe, mainly from the aquifer material. Columns with one or two reducing lenses instead experienced an increase in total acid (HNO_3)-extractable Fe, which was relatively homogeneously distributed between aquifer sediment and fined-grained, reducing lenses. However, the HCl-extractable pool of Fe shifted more dramatically than total Fe between the aquifer material and the lenses (Figure 3); fine-grained, reducing lenses exhibited a net loss of HCl-extractable Fe of 30−45%, whereas the aquifer materials immediately after a lens gained 23−69% of HCl-extractable Fe. In spite of these large shifts in HCl-extractable Fe, no differences in mineralogy were detected in X-ray diffraction (XRD) analyses of end-point samples compared to initial materials (Supporting Information Figure SI-5). This finding is consistent with the assumption that HCl-extractable Fe comprises redox-sensitive phases, such as surface-sorbed Fe(II) and poorly crystalline mackinawite, which is difficult to detect with XRD in quartz dominated materials.[17,25]

Bulk As K-edge XANES spectra from the glycerol-preserved column with three fine-grained, reducing lenses (Figure 4) show that $As(III)S_3$ complexed with organics increased in relative abundance inside reducing lenses compared to the initial material and along the flow path, at the expense of As(V). Both As(III) and As(V) were present and adsorbed to FeS in the reducing lenses. Interestingly, the As speciation in the aquifer material shifted dramatically along the flow path and compared to the initial aquifer material, which was dominated by As(V) adsorbed to Fh, with a small pool of As(III) also adsorbed to Fh (Figure 4). Before the first fine-grained reducing lens, mineral As(III)S (as realgar, As_4S_4) dominated, thereafter, As(III) adsorbed to FeS and As(V)−Fh were the dominant species with a small (but increasing along the flow path) pool of S-complexed As (represented by MTA) adsorbed to FeS. Notably, the decreasing pool of As(V) remained adsorbed to Fh, whereas the increasing pool of As(III) was adsorbed to FeS in the ports upgradient from the reduced lenses.

Similar to As, S exhibited major shifts in speciation along the flow path in the aquifer material from the glycerol-preserved column with three reducing lenses (Figure 5, left panel). Before the first lens (port 1), some zero-valent S (S^0) was detected (possibly along with some pyrite from the initial material), but no divalent sulfur (i.e., monosulfide) minerals

https://dx.doi.org/10.1021/acs.est.9b06502
Environ. Sci. Technol. 2020, 54, 3237−3244

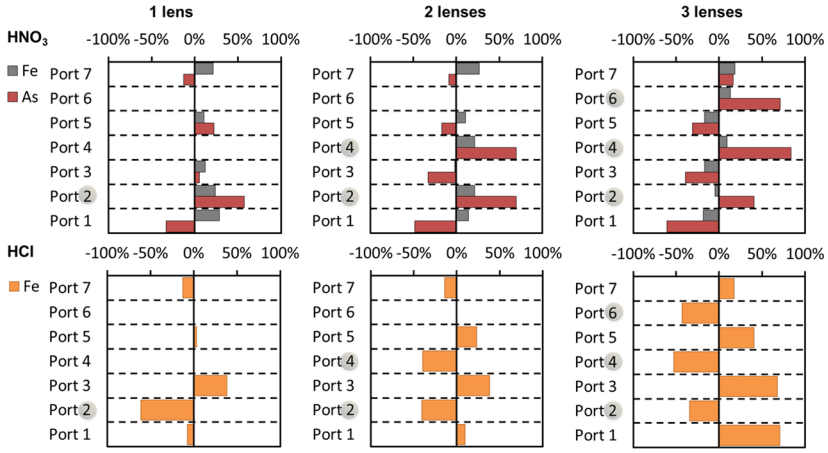

Figure 3. Estimated mass balances of total acid-extractable (70% HNO_3 digestions, top panels) Fe and As and HCl-extractable Fe (bottom panels) in columns at the end of the experiment relative to initial sediments (aquifer material for ports 1, 3, 5, and 7 and oxbow lake sediment for lenses at ports 2, 4, and 6). Estimates are based on averages for two one-lens columns and single column values for two- and three-lens columns. Positions of reducing lenses are indicated by shaded circles.

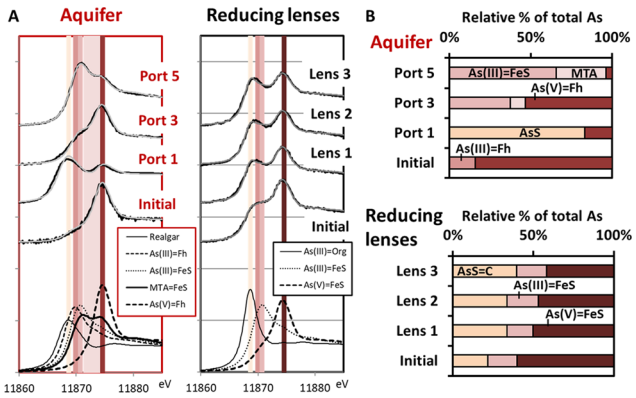

Figure 4. (A) Bulk As K-edge XANES analyses of samples from the glycerol-preserved column with three fine-grained, reducing lenses (black line) and LC-LS fits (gray line) using standard spectra (plotted at the bottom). (B) Relative distribution of As species (normalized to 100%) from the LC-LS fits; colors correspond to the vertical lines in A (indicating the absorption edge for the model compounds). Peak positions for reference spectra, data, and statistics from the fits are provided in the Supporting Information, Table SI-3.

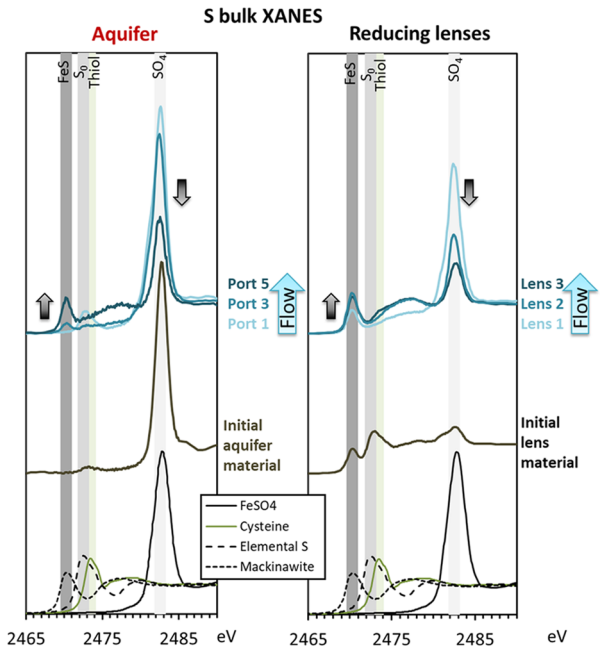

Figure 5. Sulfur K-edge XANES spectra of samples from the glycerol-preserved column with three fine-grained, reducing lenses and of initial aquifer material (left panel) and oxbow lake (lenses, right panel) materials. Arrows indicate the respective increase of mackinawite (FeS) and the decrease of sulfate along the flow path (and in relation to the initial materials). Model spectra for the dominant species are plotted at the bottom and their peak energies are indicated by vertical lines for reference: mackinawite, FeS (2470.3 eV), elemental S (S^0, 2472.5 eV), cysteine (a thiol, $C_3H_7NO_2S$, 2473.4 eV), and $FeSO_4$ (2482.6 eV).

were present. After the first lens, no S^0 was detected; instead, the relative abundance of mackinawite (FeS) increased and sulfate decreased after each fine-grained, reducing lens (ports 3 and 5). The lenses also exhibited a shift in inorganic S species from the original material containing S^0 along with FeS and sulfate to FeS and sulfate being the only detectable species at the end of the experiment and the relative abundance of FeS increasing in each lens along the flow path (Figure 5, right panel). It should be noted that there is always some uncertainty associated with the exact identification of S species from XANES, due to ~5% detection limit and multiple species exhibiting similar edge energies and spectral features. However, after taking careful consideration of the other geochemical data and comparisons of spectra from initial materials and end-point samples, as well as along the flow path, we are confident that this interpretation of the S speciation is the most plausible.

Controls on As Behavior. The combined results of aqueous (<0.15 μm colloids and dissolved species) and solid-phase speciation of As, Fe, and S reveal clear governance of redox interfaces and the relative concentrations of Fe/sulfide on the fate of As (conceptualized in the graphical abstract). A small fraction of As was likely mobilized due to the relatively high pH of the groundwater (Supporting Information, Table SI-1),[26,27] as indicated by As release in control columns (Supporting Information, Figure SI-2). However, the shifts in As speciation in relation to fine-grained, reducing lenses indicate that As behavior was dominated by redox processes. It appears that high sulfate concentrations in the groundwater, together with the abundance of microbially available organic C

https://dx.doi.org/10.1021/acs.est.9b06502
Environ. Sci. Technol. 2020, 54, 3237−3244

within fine-grained, reducing lenses (Supporting Information, Table SI-1), stimulated sulfate reduction within and along the edges of lenses to produce aqueous sulfide that dispersed within the groundwater (Figure 1). The sustained sulfide supply drove reductive dissolution of Fe(III) oxides to aqueous Fe(II), producing zero-valent S and releasing adsorbed As, as shown in previous studies.[28−33] Zero-valent S is not very stable in the aqueous phase at pH 8, where it will likely react with sulfide to form polysulfides or with other species, such as As(III), unless it is partitioned to the solid phase (as seen in the aquifer sand before the first reducing lens in this study). On the influent (upstream) side of the first fine-grained, reducing lens, it appears that aqueous Fe(II) concentrations were too low to precipitate FeS (Figure 1). Instead, the relative lack of aqueous Fe(II) (sulfide/Fe ratios >1) induced precipitation of realgar (As(III)S, As_4S_4) and zero-valent S (Figures 4 and 5), thus keeping the aqueous As concentrations relatively low. Similarly, within the fine-grained, reducing lenses, sulfide concentrations were consistently higher than the aqueous Fe concentrations (Figure SI-4) and, consequently, As(III)S species formed (Figure 4). However, due to the presence of organic matter in the lenses, As(III)S was preferentially associated with organics, probably through sulfhydryl groups,[9,34−36] and did not precipitate as realgar. This finding is consistent with the findings of Couture et al.[37] and supports the sulfurization of organics as a sink for As under sulfidic conditions.

Whether As(III)S precipitates in the mineral form or binds to sulfhydryl groups, our results show that As mobilization due to reductive dissolution is moderated when the aqueous Fe/sulfide ratio <1. Downstream of reducing lenses, aqueous Fe concentrations in the groundwater were consistently higher than the aqueous sulfide concentrations (Fe/sulfide ratios >1), which resulted in mackinawite (FeS) formation and aggregation (Figures 1, 5, and SI-4) and promoted the formation of aqueous thioarsenates (Figures 2 and 5).[27,38−43] These observations are consistent with recent findings of thioarsenates in the vicinity of reduced zones in a Bangladeshi groundwater aquifer.[11]

Although the thermodynamics and kinetics of thiolated As species and their formation are still being resolved,[44] it is clear that they (including thioarsenates) are dependent on pH and the aqueous concentrations and relative ratios of Fe, sulfide, and As.[9,39,42,45−47] In this study, the pH remained around 8 in all sampling ports (data not shown), so we assume that the observed differences in As speciation result from factors other than the pH. Further, our As concentrations (<0.5 μM) and sulfide/As ratios (>20) are considerably lower and higher, respectively, than those considered in most previous studies.[45,46,48] Thus, our findings of mixes of arsenate, arsenite, and thioarsenate species at pH 8 and in the presence of aqueous Fe(II) at molar concentrations exceeding those of sulfide are not fully consistent with published thermodynamics.[42,45,46] This is not surprising, considering the complexity of redox interfaces and nonequilibrium conditions. Nevertheless, our results clearly show that thioarsenate species can form and remain stable under our experimental conditions, indicating that at pH 8, a mixture of aqueous thioarsenates form when sulfide is present at sulfide/As ratios <100 and sulfide/Fe(II) ratios <1. If sulfide/As ratios exceed 100 and sulfide/Fe(II) ratios exceed 1, As−S interactions instead partition As to the solid phase as realgar and/or organically complexed As(III)S. We found no evidence of orpiment (As_2S_3) in the solid phase As K-edge XANES spectra (Figure 4), despite its common occurrence and thermodynamic stability over a wide range of conditions in comparison to realgar.[45,46] However, orpiment does exhibit a higher solubility at neutral to alkaline pH[45] and realgar has previously been found in natural sediments[34,40,49] and laboratory experiments.[35,48,50] The precipitation of mineral As−S only at sulfide/As ratios above 100 is inconsistent with previous studies[49,51] and is likely the result of the considerably higher pH in the current study where aqueous thioarsenates are more favorable.[42,45,46,52]

The presence of S-complexed As species in both aqueous (thioarsenates) and solid (adsorbed to organics and FeS) phases in this experiment adds to the increasing evidence for the importance of these species in sulfidic environments.[11,12,43] Further, the fact that thioarsenates were most abundant in samples with high aqueous As concentrations suggests that thiolation promotes As mobilization, as has been proposed by others.[9,14,53] Thus, as previously found for bioamended sediments,[29] our results indicate that aquifers with low (<2 mg/kg) sediment concentrations of As may be at risk for groundwater As concentrations exceeding the drinking water standards (10 μg/L) if the formation of thiolated As species is favorable, i.e., under dominant Fe-reducing conditions with a low, but consistent, supply of sulfide and near-neutral pH.

Importantly, here the influence of sulfate-reducing zones on groundwater chemistry extended downgradient from the fine-grained, reducing lenses at distances up to four times the diameter of the lens itself. Although we only used one size and shape of reduced lenses, this suggests that relatively small layers or lenses of fine-grained, reducing material can have an outsized influence on otherwise oxic aquifers. Unfortunately, borehole samples and geology-based assessments that are performed prior to well installations are typically conducted on a scale where the presence of fine-grained, reducing lenses (i.e., redox heterogeneities) can easily be missed (or their presence is disregarded). Thus, future studies should investigate the relevance of dimensions and spacing of redox heterogeneities induced by fine-grained, reduced lenses on their influence on groundwater chemistry. Such data, and the data from this study, provide guidance for developing predictive groundwater quality models for aquifers exhibiting heterogeneous sediment composition (cf. ref 6).

■ ASSOCIATED CONTENT

Supporting Information

The Supporting Information is available free of charge at https://pubs.acs.org/doi/10.1021/acs.est.9b06502.

Schematic of column design; initial concentrations of relevant elements and particle size distribution in natural sediments used for the experiment; groundwater chemical composition; aqueous concentrations of As, Fe, and sulfide in groundwater ports (1, 3, 5, and 7) on day 35 and day 70 of the experiment; temporal evolution of aqueous sulfide, Fe, and As in the groundwater in control columns (without reducing lenses) and pore-water inside reducing lenses; diffractograms from initial and end-point samples of aquifer material and reducing lens material; details from As and SK-edge XANES analyses (PDF)

https://dx.doi.org/10.1021/acs.est.9b06502
Environ. Sci. Technol. 2020, 54, 3237−3244

AUTHOR INFORMATION

Corresponding Author

Kristin Boye − *Geochemistry and Biogeochemistry Group, SLAC National Accelerator Laboratory, Menlo Park, California 94025, United States;* orcid.org/0000-0003-2087-607X; Email: kboye@slac.stanford.edu

Authors

Naresh Kumar − *Department of Geological Sciences, Stanford University, Stanford, California 94305-2115, United States; Department of Environmental Geosciences, Centre for Microbiology and Environmental Systems Science, University of Vienna, 1090 Vienna, Austria*

Vincent Noël − *Geochemistry and Biogeochemistry Group, SLAC National Accelerator Laboratory, Menlo Park, California 94025, United States;* orcid.org/0000-0002-5387-8664

Britta Planer-Friedrich − *Environmental Geochemistry, Bayreuth Center for Ecology and Environmental Research (BayCEER), University of Bayreuth, D-95440 Bayreuth, Germany;* orcid.org/0000-0002-0656-4283

Johannes Besold − *Environmental Geochemistry, Bayreuth Center for Ecology and Environmental Research (BayCEER), University of Bayreuth, D-95440 Bayreuth, Germany*

Juan Lezama-Pacheco − *Department of Earth System Science, Stanford University, Stanford, California 94305-4216, United States*

John R. Bargar − *Geochemistry and Biogeochemistry Group, SLAC National Accelerator Laboratory, Menlo Park, California 94025, United States;* orcid.org/0000-0001-9303-4901

Gordon E. Brown, Jr. − *Department of Geological Sciences, Stanford University, Stanford, California 94305-2115, United States; Department of Photon Science, SLAC National Accelerator Laboratory, Menlo Park, California 94025, United States*

Scott Fendorf − *Department of Earth System Science, Stanford University, Stanford, California 94305-4216, United States;* orcid.org/0000-0002-9177-1809

Complete contact information is available at: https://pubs.acs.org/10.1021/acs.est.9b06502

Notes

The authors declare no competing financial interest.

ACKNOWLEDGMENTS

This work was funded by the U.S. Department of Energy (DOE), Office of Science, Office of Biological and Environmental Research (BER), through the SLAC National Accelerator Laboratory scientific focus area (SFA) (Contract No. DE-AC02-76SF00515). Work by N.K. and G.E.B. was supported by the U.S. National Science Foundation and the U.S. Environmental Protection Agency under NSF Cooperative Agreement EF-0830093, to the Center for the Environmental Implications of NanoTechnology (CEINT), based at Duke University. Work by S.F. was supported by the U.S. DOE BER Subsurface Biogeochemistry Program (Award Number DE-SC0020205). B.P.F. and J.B. were supported by the German Research Foundation Grant PL 302/20-1. Use of the Stanford Synchrotron Radiation Lightsource, SLAC National Accelerator Laboratory, is supported by the U.S. DOE, Office of Science, Office of Basic Energy Sciences under Contract No. DE-AC02-76SF00515. This study could not have been completed without sampling and analytical efforts provided by the following people: George Sims, Dustin Proctor (Central Wyoming College); Laura E. Spielman, Lilia Barragan, Guangchao Li, and Douglas Turner (Stanford University).

REFERENCES

(1) Fakhreddine, S.; Dittmar, J.; Phipps, D.; Dadakis, J.; Fendorf, S. Geochemical triggers of arsenic mobilization during managed aquifer recharge. *Environ. Sci. Technol.* **2015**, *49*, 7802−7809.

(2) Fendorf, S.; Nico, P. S.; Kocar, B. D.; Masue, Y.; Tufano, K. J. Arsenic Chemistry in Soils and Sediments. In *Developments in Soil Science*; Elsevier, 2010; Vol. *34*, pp 357−378.

(3) Smedley, P. L.; Kinniburgh, D. A review of the source, behaviour and distribution of arsenic in natural waters. *Appl. Geochem.* **2002**, *17*, 517−568.

(4) Foster, A. L.; Kim, C. S. Arsenic speciation in solids using X-ray absorption spectroscopy. *Rev. Mineral. Geochem.* **2014**, *79*, 257−369.

(5) Fendorf, S.; Michael, H. A.; van Geen, A. Spatial and Temporal Variations of Groundwater Arsenic in South and Southeast Asia. *Science* **2010**, *328*, 1123.

(6) Fakhreddine, S.; Lee, J.; Kitanidis, P. K.; Fendorf, S.; Rolle, M. Imaging geochemical heterogeneities using inverse reactive transport modeling: An example relevant for characterizing arsenic mobilization and distribution. *Adv. Water Resour.* **2016**, *88*, 186−197.

(7) Mirecki, J. E.; Bennett, M. W.; López-Baláez, M. C. Arsenic control during aquifer storage recovery cycle tests in the Floridan Aquifer. *Groundwater* **2013**, *51*, 539−549.

(8) Prommer, H.; Stuyfzand, P. J. Identification of temperature-dependent water quality changes during a deep well injection experiment in a pyritic aquifer. *Environ. Sci. Technol.* **2005**, *39*, 2200−2209.

(9) Besold, J.; Biswas, A.; Suess, E.; Scheinost, A. C.; Rossberg, A.; Mikutta, C.; Kretzschmar, R.; Gustafsson, J. P.; Planer-Friedrich, B. Monothioarsenate Transformation Kinetics Determining Arsenic Sequestration by Sulfhydryl Groups of Peat. *Environ. Sci. Technol.* **2018**, *52*, 7317−7326.

(10) Planer-Friedrich, B.; London, J.; McCleskey, R. B.; Nordstrom, D. K.; Wallschläger, D. Thioarsenates in geothermal waters of Yellowstone National Park: determination, preservation, and geochemical importance. *Environ. Sci. Technol.* **2007**, *41*, 5245−5251.

(11) Planer-Friedrich, B.; Schaller, Jr.; Wismeth, F.; Mehlhorn, J.; Hug, S. J. Monothioarsenate Occurrence in Bangladesh Groundwater and Its Removal by Ferrous and Zero-Valent Iron Technologies. *Environ. Sci. Technol.* **2018**, *52*, 5931−5939.

(12) Planer-Friedrich, B.; Suess, E.; Scheinost, A. C.; Wallschläger, D. Arsenic speciation in sulfidic waters: reconciling contradictory spectroscopic and chromatographic evidence. *Anal. Chem.* **2010**, *82*, 10228−10235.

(13) Beak, D. G.; Wilkin, R. T. Performance of a Zerovalent iron reactive barrier for the treatment of arsenic in groundwater: Part 2. Geochemical modeling and solid phase studies. *J. Contam. Hydrol.* **2009**, *106*, 15−28.

(14) Stucker, V. K.; Silverman, D. R.; Williams, K. H.; Sharp, J. O.; Ranville, J. F. Thioarsenic species associated with increased arsenic release during biostimulated subsurface sulfate reduction. *Environ. Sci. Technol.* **2014**, *48*, 13367−13375.

(15) Boye, K.; Noël, V.; Tfaily, M. M.; Bone, S. E.; Williams, K. H.; Bargar, J. R.; Fendorf, S. Thermodynamically controlled preservation of organic carbon in floodplains. *Nat. Geosci.* **2017**, *10*, 415.

(16) Janot, N.; Lezama Pacheco, J. S.; Pham, D. Q.; O'Brien, T. M.; Hausladen, D.; Noël, V.; Lallier, F.; Maher, K.; Fendorf, S.; Williams, K. H.; et al. Physico-chemical heterogeneity of organic-rich sediments in the Rifle aquifer, CO: Impact on uranium biogeochemistry. *Environ. Sci. Technol.* **2016**, *50*, 46−53.

(17) Noël, V.; Boye, K.; Kukkadapu, R. K.; Bone, S.; Pacheco, J. S. L.; Cardarelli, E.; Janot, N.; Fendorf, S.; Williams, K. H.; Bargar, J. R. Understanding controls on redox processes in floodplain sediments of the Upper Colorado River Basin. *Sci. Total Environ.* **2017**, *603−604*, 663−675.

(18) Noël, V.; Boye, K.; Lezama Pacheco, J. S.; Bone, S. E.; Janot, Nm.; Cardarelli, E.; Williams, K. H.; Bargar, J. R. Redox controls over the stability of U (IV) in floodplains of the Upper Colorado River Basin. *Environ. Sci. Technol.* **2017**, *51*, 10954−10964.
(19) Campbell, K. M.; Kukkadapu, R. K.; Qafoku, N.; Peacock, A. D.; Lesher, E.; Williams, K. H.; Bargar, J. R.; Wilkins, M. J.; Figueroa, L.; Ranville, J.; et al. Geochemical, mineralogical and microbiological characteristics of sediment from a naturally reduced zone in a uranium-contaminated aquifer. *Appl. Geochem.* **2012**, *27*, 1499−1511.
(20) Qafoku, N. P.; Kukkadapu, R. K.; McKinley, J. P.; Arey, B. W.; Kelly, S. D.; Wang, C.; Resch, C. T.; Long, P. E. Uranium in framboidal pyrite from a naturally bioreduced alluvial sediment. *Environ. Sci. Technol.* **2009**, *43*, 8528−8534.
(21) Plafcan, M.; Eddy-Miller, C. A.; Ritz, G. F.; Holland Ii, J. P. R.; Stockdale, R. G. *Water Resources of Fremont County, Wyoming*; Water-Resources Investigations Report 95-4095, 1995.
(22) Cline, J. D. Spectrophotometric determination of hydrogen sulfide in natural waters 1. *Limnol. Oceanogr.* **1969**, *14*, 454−458.
(23) Viollier, E.; Inglett, P.; Hunter, K.; Roychoudhury, A.; Van Cappellen, P. The ferrozine method revisited: Fe (II)/Fe (III) determination in natural waters. *Appl. Geochem.* **2000**, *15*, 785−790.
(24) Newville, M.; Ravel, B. HEPHAESTUS: data analysis for x-ray absorption spectroscopy using Ifeffit Ravel, B.; Newville, M. *J. Synchrotron Radiat.* **2005**, *12*, 537−541.
(25) Noël, V.; Boye, K.; Kukkadapu, R. K.; Li, Q.; Bargar, J. R. Uranium storage mechanisms in wet-dry redox cycled sediments. *Water Res.* **2019**, *152*, 251−263.
(26) Antelo, J.; Avena, M.; Fiol, S.; López, R.; Arce, F. Effects of pH and ionic strength on the adsorption of phosphate and arsenate at the goethite−water interface. *J. Colloid Interface Sci.* **2005**, *285*, 476−486.
(27) Wolthers, M.; Charlet, L.; van Der Weijden, C. H.; van der Linde, P. R.; Rickard, D. Arsenic mobility in the ambient sulfidic environment: Sorption of arsenic(V) and arsenic(III) onto disordered mackinawite. *Geochim. Cosmochim. Acta* **2005**, *69*, 3483−3492.
(28) Poulton, S. W.; Krom, M. D.; Raiswell, R. A revised scheme for the reactivity of iron (oxyhydr)oxide minerals towards dissolved sulfide. *Geochim. Cosmochim. Acta* **2004**, *68*, 3703−3715.
(29) Smith, S.; Dupont, R. R.; McLean, J. E. Arsenic Release and Attenuation Processes in a Groundwater Aquifer During Anaerobic Remediation of TCE with Biostimulation. *Groundwater Monit. Rem.* **2019**, *39*, 61−70.
(30) Kumar, N.; Lezama Pacheco, J.; Noël, V.; Dublet, G.; Brown, G. E. sulfidation mechanisms of Fe(iii)-(oxyhydr)oxide nanoparticles: a spectroscopic study. *Environ. Sci.: Nano* **2018**, *5*, 1012−1026.
(31) Peiffer, S.; Wan, M. Reductive Dissolution and Reactivity of Ferric (Hydr)oxides: New Insights and Implications for Environmental Redox Processes. In *Iron Oxides: From Nature to Applications*; Wiley-VCH Verlag GmbH & Co. KGaA: Weinheim, Germany, 2016.
(32) Hellige, K.; Pollok, K.; Larese-Casanova, P.; Behrends, T.; Peiffer, S. Pathways of ferrous iron mineral formation upon sulfidation of lepidocrocite surfaces. *Geochim. Cosmochim. Acta* **2012**, *81*, 69−81.
(33) Pyzik, A. J.; Sommer, S. E. Sedimentary iron monosulfides: kinetics and mechanism of formation. *Geochim. Cosmochim. Acta* **1981**, *45*, 687−698.
(34) Langner, P.; Mikutta, C.; Kretzschmar, R. Arsenic sequestration by organic sulphur in peat. *Nat. Geosci.* **2012**, *5*, 66.
(35) Langner, P.; Mikutta, C.; Suess, E.; Marcus, M. A.; Kretzschmar, R. Spatial Distribution and Speciation of Arsenic in Peat Studied with Microfocused X-ray Fluorescence Spectrometry and X-ray Absorption Spectroscopy. *Environ. Sci. Technol.* **2013**, *47*, 9706−9714.
(36) Hoffmann, M.; Mikutta, C.; Kretzschmar, R. Bisulfide Reaction with Natural Organic Matter Enhances arsenite Sorption: Insights from X-ray Absorption Spectroscopy. *Environ. Sci. Technol.* **2012**, *46*, 11788−11797.
(37) Couture, R.-M.; Wallschläger, D.; Rose, J.; Van Cappellen, P. Arsenic binding to organic and inorganic sulfur species during microbial sulfate reduction: a sediment flow-through reactor experiment. *Environ. Chem.* **2013**, *10*, 285−294.
(38) Burton, E. D.; Johnston, S. G.; Bush, R. T. Microbial sulfidogenesis in ferrihydrite-rich environments: Effects on iron mineralogy and arsenic mobility. *Geochim. Cosmochim. Acta* **2011**, *75*, 3072−3087.
(39) Vega, A. S.; Planer-Friedrich, B.; Pastén, P. A. arsenite and arsenate immobilization by preformed and concurrently formed disordered mackinawite (FeS). *Chem. Geol.* **2017**, *475*, 62−75.
(40) O'Day, P. A.; Vlassopoulos, D.; Root, R.; Rivera, N. The influence of sulfur and iron on dissolved arsenic concentrations in the shallow subsurface under changing redox conditions. *Proc. Natl. Acad. Sci. U.S.A.* **2004**, *101*, 13703−13708.
(41) Couture, R. M.; Rose, J.; Kumar, N.; Mitchell, K.; Wallschläger, D.; Van Cappellen, P. Sorption of arsenite, Arsenate, and Thioarsenates to Iron Oxides and Iron Sulfides: A Kinetic and Spectroscopic Investigation. *Environ. Sci. Technol.* **2013**, *47*, 5652−5659.
(42) Couture, R.-M.; Van Cappellen, P. Reassessing the role of sulfur geochemistry on arsenic speciation in reducing environments. *J. Hazard. Mater.* **2011**, *189*, 647−652.
(43) Stauder, S.; Raue, B.; Sacher, F. Thioarsenates in sulfidic waters. *Environ. Sci. Technol.* **2005**, *39*, 5933−5939.
(44) Herath, I.; Vithanage, M.; Seneweera, S.; Bundschuh, J. Thiolated arsenic in natural systems: What is current, what is new and what needs to be known. *Environ. Int.* **2018**, *115*, 370−386.
(45) Wilkin, R. T.; Wallschläger, D.; Ford, R. G. Speciation of arsenic in sulfidic waters. *Geochem. Trans.* **2003**, *4*, No. 1.
(46) Helz, G. R.; Tossell, J. A. Thermodynamic model for arsenic speciation in sulfidic waters: A novel use of ab initio computations. *Geochim. Cosmochim. Acta* **2008**, *72*, 4457−4468.
(47) Wood, S. A.; Tait, C. D.; Janecky, D. R. A Raman spectroscopic study of arsenite and thioarsenite species in aqueous solution at 25 C. *Geochem. Trans.* **2002**, *3*, 31.
(48) Bostick, B. C.; Fendorf, S.; Brown, G. E. In situ analysis of thioarsenite complexes in neutral to alkaline arsenic sulphide solutions. *Mineral. Mag.* **2005**, *69*, 781.
(49) Root, R. A.; Vlassopoulos, D.; Rivera, N. A.; Rafferty, M. T.; Andrews, C.; O'Day, P. A. Speciation and natural attenuation of arsenic and iron in a tidally influenced shallow aquifer. *Geochim. Cosmochim. Acta* **2009**, *73*, 5528−5553.
(50) Gallegos, T. J.; Han, Y.-S.; Hayes, K. F. Model predictions of realgar precipitation by reaction of As (III) with synthetic mackinawite under anoxic conditions. *Environ. Sci. Technol.* **2008**, *42*, 9338−9343.
(51) Rochette, E. A.; Bostick, B. C.; Li, G.; Fendorf, S. Kinetics of Arsenate Reduction by Dissolved Sulfide. *Environ. Sci. Technol.* **2000**, *34*, 4714−4720.
(52) Planer-Friedrich, B.; Wallschläger, D. A critical investigation of hydride generation-based arsenic speciation in sulfidic waters. *Environ. Sci. Technol.* **2009**, *43*, 5007−5013.
(53) Kumar, N.; Couture, R.-M.; Millot, R.; Battaglia-Brunet, F.; Rose, J. Microbial Sulfate Reduction Enhances Arsenic Mobility Downstream of Zerovalent-Iron-Based Permeable Reactive Barrier. *Environ. Sci. Technol.* **2016**, *50*, 7610−7617.

https://dx.doi.org/10.1021/acs.est.9b06502
Environ. Sci. Technol. 2020, 54, 3237−3244